RESEARCH

Open Access

Skewed alpha-stable distribution for natural texture modeling and segmentation in contourlet domain

Katayoon Sarafrazi[1*] (iD) and Mehran Yazdi[2]

Abstract

Texture modeling is a very useful tool in image analysis. This model can be used in texture segmentation, denoising or texture synthesis. In this work, alpha-stable distribution has been proposed to model and segment textured images in contourlet domain. Contourlet transform's ability to extract texture features in different scales and directions combined with alpha-stable distribution's modeling capabilities prove to be an effective method for texture feature extraction. Kolmogorov–Smirnov distance has been used to evaluate how well the proposed distribution fits to the image in the contourlet domain. The performance of the proposed features on image segmentation has been also compared with that of features extracted using different texture analysis methods in the presence of noise. Experimental results have demonstrated the superior performance of the proposed features and their robust performance in the presence of noise.

Keywords: Alpha-stable distribution, Contourlet transform, Image segmentation, Texture modeling

1 Introduction

Over the recent years, texture analysis and modeling have been a hot topic in the field of image processing. Texture synthesis, texture retrieval, denoising of textured images, edge detection in textured images, and texture segmentation are some of the most important challenges in this domain. Having an accurate statistical model for textured images can be very useful to deal with these challenges, especially image segmentation.

Texture segmentation is dividing the image into regions with similar texture. Segmenting a textured image is a challenging task because using traditional segmentation methods in textured images often results in an over segmentation [1]. This is due to the fact that a textured region usually consists of many small homogeneous regions (texture elements). Traditional segmentation methods rely on the pixel value for segmentation while an efficient texture analysis method should consider its neighboring pixel values too.

In this paper, different distributions have been used for modeling and segmentation of textured natural images in contourlet domain. Skewed alpha-stable distribution which is a generalized form of Rayleigh distribution presents the best results. The proposed method's performance is also compared to other algorithms. Simulation results show superiority of the proposed algorithm related to the other methods.

2 Literature review

Feature extraction is the most important step in texture segmentation. Having some texture discriminative descriptors can make the segmentation process straightforward. Therefore, various works in recent years have been carried out in texture feature extraction [1–9]. Texture analysis methods can be divided

* Correspondence: Sarafrazi@shirazu.ac.ir; katayoon_sarafrazi@yahoo.com
[1]Shiraz University, Shiraz, Iran
Full list of author information is available at the end of the article

Fig. 1 Contourlet transform

**Fig. 3** Alpha-stable distribution for different values of β
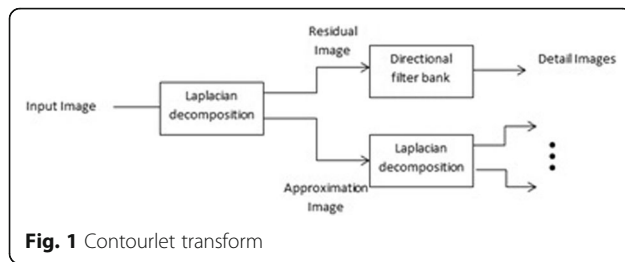
into four categories: statistical methods (e.g., co-occurrence matrices [10–12], autocorrelation features [13, 14]), geometrical methods (e.g., Voronoi tessellations [15, 16]), model base methods (e.g., random fields [5, 17–19], fractals [12, 20]) and signal processing methods (e.g., spatial domain filtering [21, 22], Fourier domain filtering [2], and wavelet-based methods [16, 23]).

Statistical modeling is one of the most popular texture analysis methods. In this approach, the pixel values are assumed to be random variables drawn from a specific distribution, then the distribution's parameters are estimated and can be used as features in different tasks such as image segmentation [24–26] or denoising [27]. Various distributions have been used for texture modeling and segmentation. Gaussian distribution is one of the most commonly used models for texture analysis [24, 28, 29]. Rayleigh, Weibull [30, 31], and Wishart [25] distributions have been also used for texture feature extraction. However, due to its shape and properties, each of these distributions is suitable for a specific type of data. For example, Rayleigh and Gaussian distributions are unable to fit heavy-tailed or nonsymmetrical
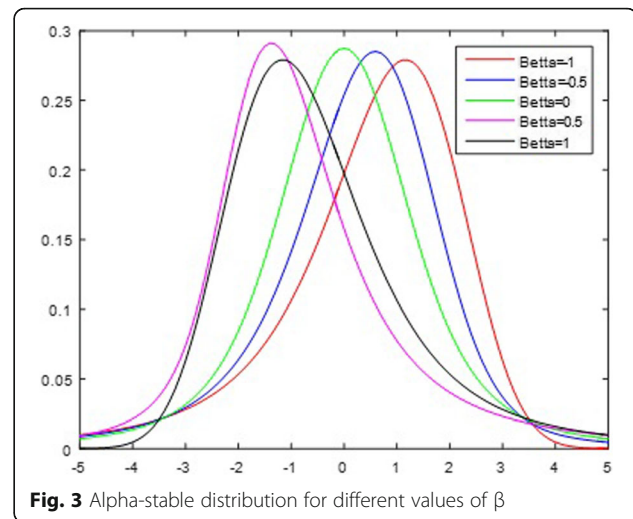
histograms. To solve this problem, we propose using alpha-stable distribution for texture modeling. Alpha-stable or Levy distributions firstly introduced by Levy [25] are a family of distributions which are able to model a wide range of data; this is because in its general form, alpha-stable distribution can be asymmetric having various shapes.

Many researchers have used texture modeling and feature extraction in multiresolution domains like wavelet transform [26, 27]. Most of these methods use transform coefficients' energy [28], fractal dimension [20], or statistical modeling parameters [29–31] as texture features. Different multiresolution transforms have been introduced in recent years. Wavelet transform is the simplest and most popular one used for texture feature extraction. Wavelet's advantages
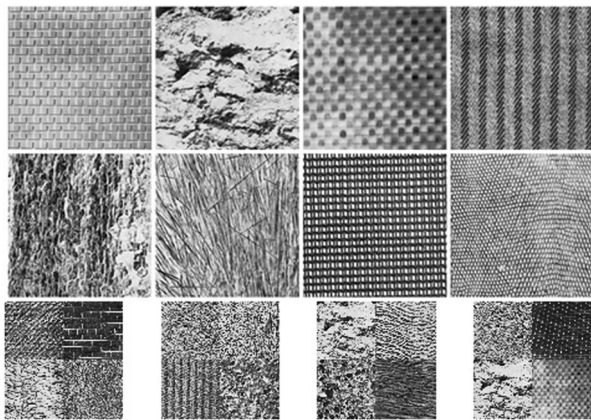

Fig. 2 Alpha-stable distribution for different values of α

Fig. 4 Alpha-stable distribution for different values of γ
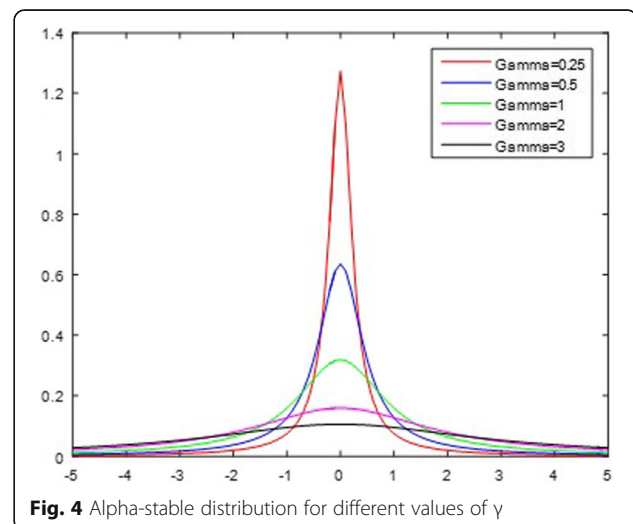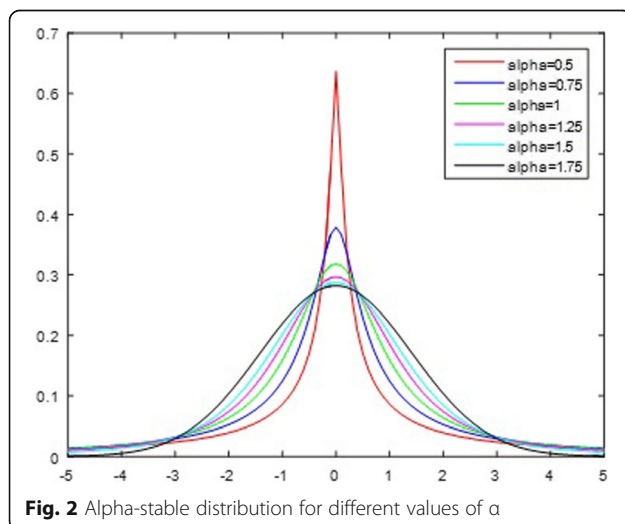
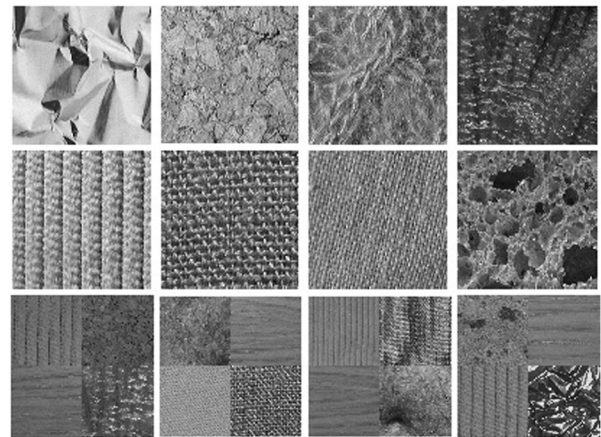**Fig. 5** Texture samples from Brodatz album

Fig. 7 Texture samples from the KTH-TIPS2 database

are simplicity and low redundancy but decomposing in these two directions is its serious disadvantage that limits the number of informative features extracted from the image. Contourlet transform has been introduced to overcome this problem. Contourlet [32] is a two-dimensional transform that uses a pyramidal directional filter bank to extract image details at different scale and directions. Since there is no limitation on the number of directions in contourlet, various texture features can be extracted.

Statistical modeling in transform domain is one of the most effective texture feature extraction and classification methods. For example, Euclidean or Kullback-Liebler distance between the distributions can be used as a similarity measurement for texture classification [29, 33], or the distribution's parameters can be used as texture features [29]. Different distributions have been used to model texture in the multiresolution domain. Generalized-Gaussian distribution has been used to model wavelet [29, 34, 35] and contourlet [31] coefficients. Kwitt and Uhl [36] have used gamma and Weibull distributions to model texture in complex DWT domain. Generalized gamma distribution has been also used for texture modeling in transform domain [37, 38].

In our work, alpha-stable distribution is proposed to model and segment textured images in contourlet domain. We have used the alpha-stable parameters of these detail images for texture segmentation. Contourlet transform's ability to extract texture features in different scales and directions combined with alpha-stable distribution's modeling capabilities prove to be an effective method for texture analysis and feature extraction. Simulation results show that a significant improvement has been achieved by this method compared with other texture segmentation methods.
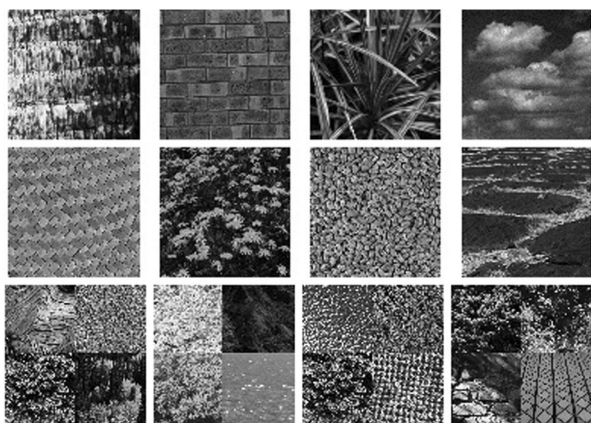

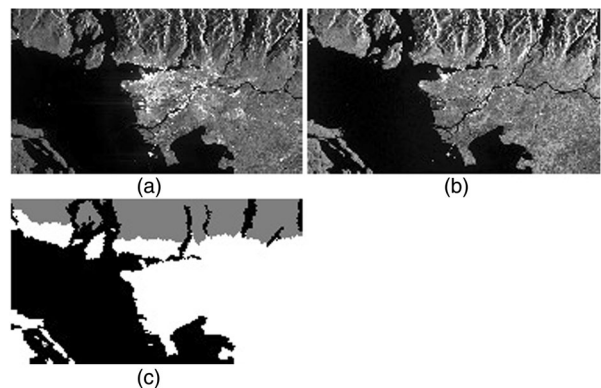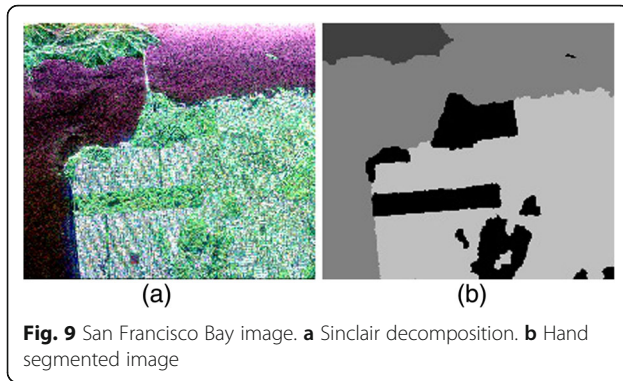**Fig. 6** Texture samples from Vistex album

Fig. 8 Vancouver image. **a** HH band. **b** HV band. **c** Hand segmented image

Fig. 9 San Francisco Bay image. **a** Sinclair decomposition. **b** Hand segmented image

Table 1 Used feature sets in our work

	Method	Number of features
Feature set 1	Gaussian distribution [24, 46]	2
Feature set 2	Rayleigh distribution [42]	1
Feature set 3	Alpha-stable distribution	4
Feature set 4	Gaussian distribution of contourlet subbands	66
Feature set 5	Rayleigh distribution of contourlet subbands	33
Feature set 6	Alpha-stable distribution of contourlet subbands	132
Feature set 7	Fractal dimension [20]	1
Feature set 8	Fractal dimension of contourlet subbands [20]	33
Feature set 9	Alpha-stable distribution of wavelet subbands	16

3 Contourlet transform

Recently, wavelet transform has been widely used in signal processing. This is because wavelet transform provides a good nonlinear approximation for piecewise smooth functions in one dimension [39]. However, since two-dimensional wavelet is the tensor product of one-dimensional wavelet, it can only model zero-dimension discontinuities (points). On the other hand, in an image, edges are one-dimension discontinuities and thus cannot be modeled using wavelets. Contourlet transform is a "true two-dimensional representation of images which can capture the intrinsic geometrical structure inherent in visual information" [32].

Contourlet transform uses a multiscale filter bank like Laplacian that performs the pyramid decomposition. On each decomposition level, the prediction residual image is passed through a directional filter bank to calculate details in different directions. Figure 1 shows the block diagram for Contourlet transform.

In our work, we use Contourlet transform's ability to extract image details in various scales and directions to build a strong texture descriptor.

4 Skewed alpha-stable distribution

The concept of stable distributions was firstly introduced by levy [25]. This family of distributions does not have a close formed probability density function and is defined by a characteristic function which is shown in Eq. 1.
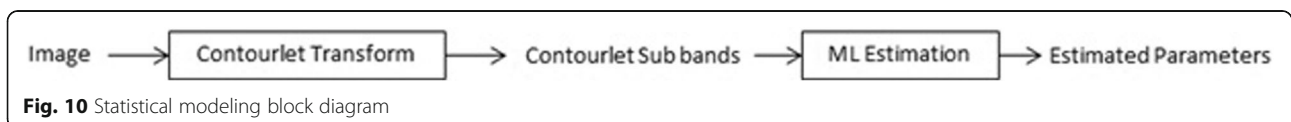
$$
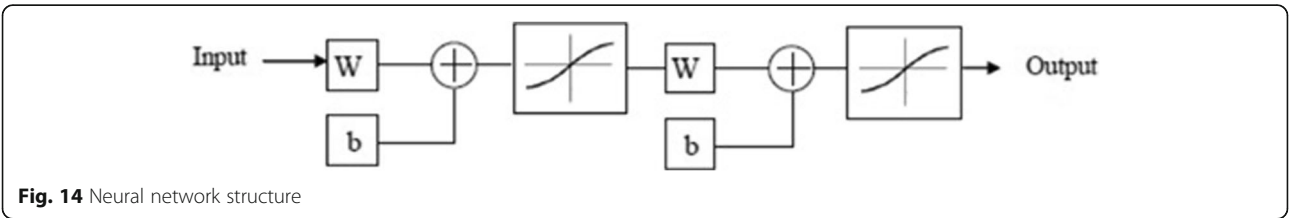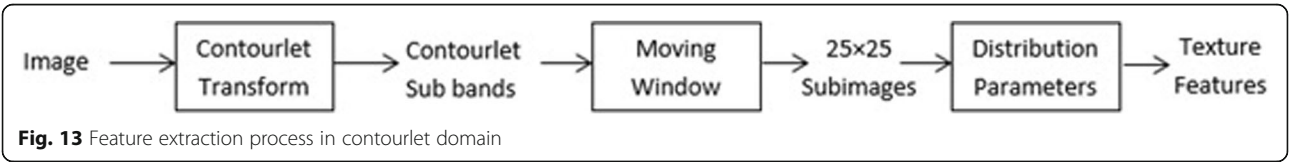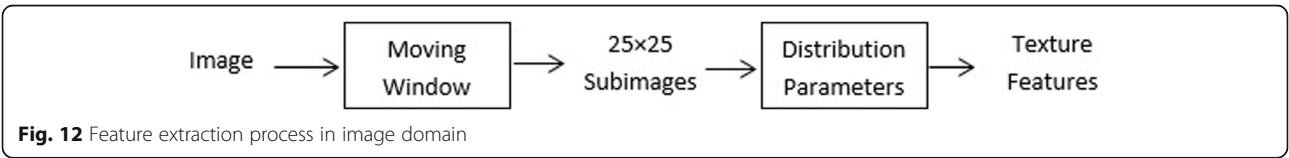\phi(\omega) = \begin{cases} \exp\left\{ j\mu\omega - |\gamma\omega|^{\alpha}\left[1 - jsgn(\omega)\beta\,\tan\left(\frac{\pi\alpha}{2}\right)\right]\right\}, \alpha \neq 1 \\ \exp\left\{ j\mu\omega - |\gamma\omega|\left[1 + jsgn(\omega)\beta\frac{2}{\pi}\,\ln(\omega)\right]\right\}, \alpha \neq 1 \end{cases}
$$

$$(1)$$

Probability density function can be obtained by taking FFT (fast Fourier transform) of the characteristic function. Alpha-stable distribution has four parameters: $\alpha \in (0, 2]$ (shape parameter), $\beta \in [-1, 1]$ (skewness parameter), $\gamma \in \mathbb{R}^{+}$ (dispersion parameter), and $\mu \in \mathbb{R}$ (location parameter). Gaussian distribution is a special case of alpha-stable distribution with $\alpha = 2$. Figures 2, 3, and 4 show the alpha-stable probability density function for different values of α, β, and γ.

Due to its flexibility in representing heavy-tailed and non-symmetric data, alpha stable distribution can be used to model a wide range of texture data. Combining this with contourlet's ability to extract texture features in different scales and directions gives us a full texture descriptor.
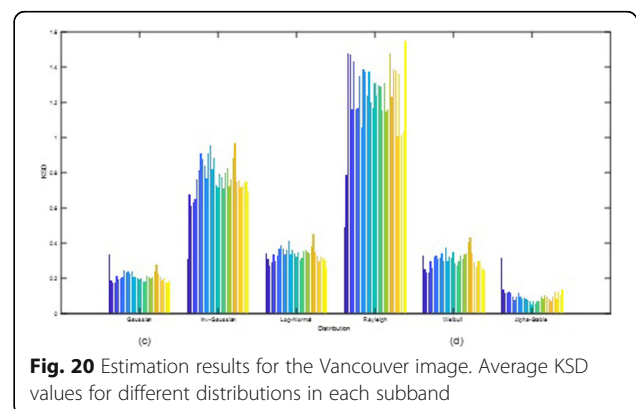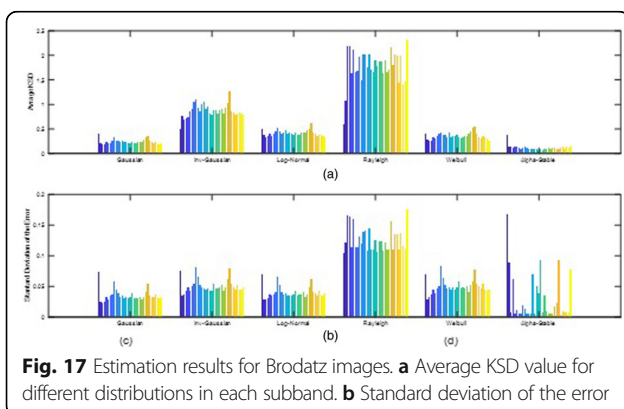

Fig. 10 Statistical modeling block diagram

Fig. 11 Segmentation algorithm

Fig. 12 Feature extraction process in image domain

Fig. 13 Feature extraction process in contourlet domain

Fig. 14 Neural network structure

Fig. 15 Hyperbolic tangent sigmoid transfer function

Fig. 18 Estimation results for Vistex images. **a** Average KSD value for different distributions in each subband. **b** Standard deviation of the error

Fig. 16 Average KSD values of each contourlet subband for the alpha-stable distribution. **a** Brodatz album. **b** Vistex database. **c** KTH-TIPS2 database. **d** Vancouver area image. **e** San Francisco Bay area

Fig. 19 Estimation results for KTH database images. **a** Average KSD value for different distributions in each subband. **b** Standard deviation of the error

Fig. 17 Estimation results for Brodatz images. **a** Average KSD value for different distributions in each subband. **b** Standard deviation of the error

Fig. 20 Estimation results for the Vancouver image. Average KSD values for different distributions in each subband
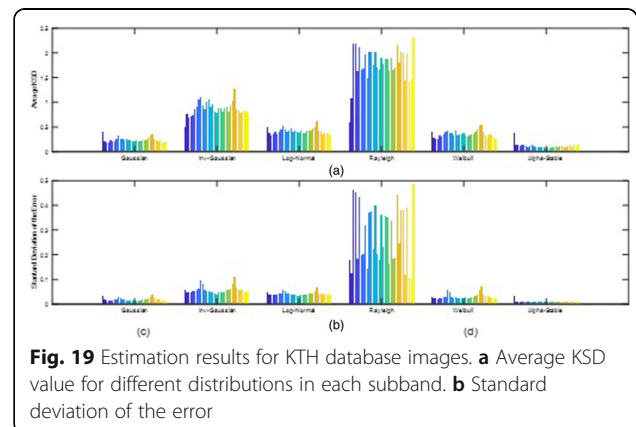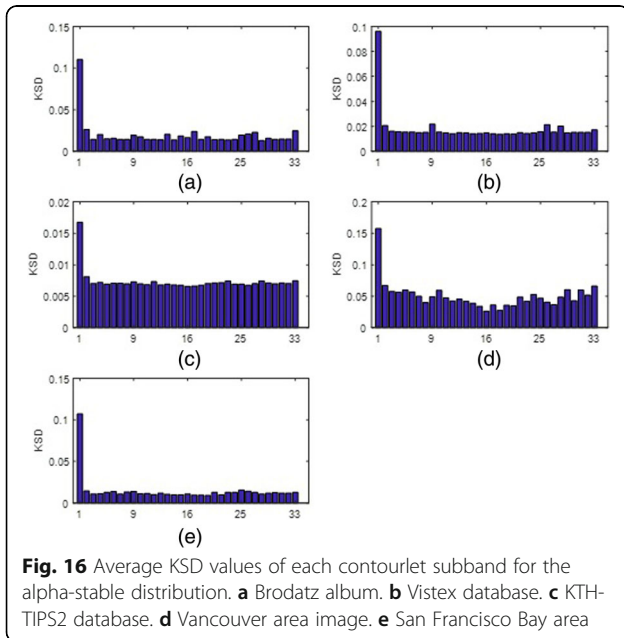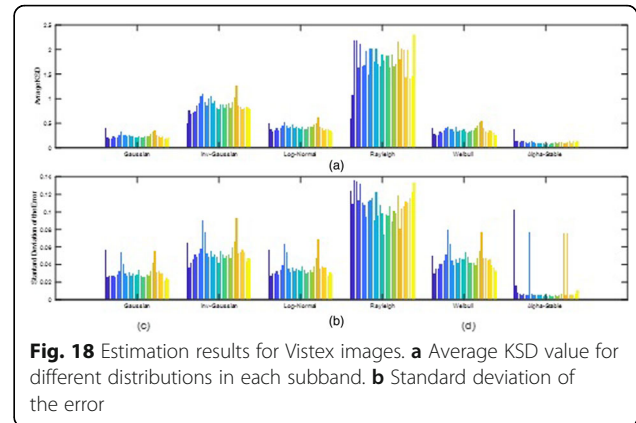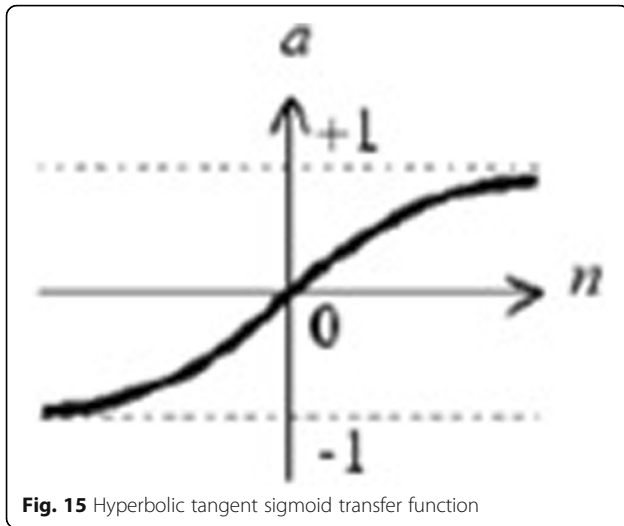
Table 2 Average segmentation accuracy of different methods (without noise)

	Gaussian	Rayleigh	Alpha-Stable	Contourlet + Gaussian	Contourlet + Rayleigh	Contourlet + alpha-stable	Fractal	Contourlet + Fractal	Wavelet + alpha-stable
Brodatz album	36.19	35.26	35.15	98.92	99.39	99.50	40.92	65.52	98.71
Vistex Database	40.65	35.56	35.40	99.01	99.43	99.53	44.69	64.71	98.85
KTH-TIPS2	34.00	32.48	32.60	99.04	99.40	99.48	37.47	56.53	98.91
Vancouver	86.16	81.24	89.79	95.40	74.40	96.19	84.16	66.25	61.08
San Francisco Bay	94.07	89.87	91.03	98.29	97.17	98.62	91.65	88.37	85.56

5 Materials and method

In simulation process, different texture mosaics from Brodatz album [40], Vistex database, and the KTH-TIPS2 database [41] which contain multiple natural textures, in addition to two polarimetric SAR images, have been used. These polarimetric images consist of a RADARSAT-2 image of Vancouver area and an AIRSAR image of San Francisco Bay.

In segmentation process, 100 random texture mosaics containing textures from Brodatz, Vistex, or the KTH-TIPS2 album have been used. Figure 5 shows some sample texture and mosaics from Brodatz album. Figure 6 contains textures from Vistex database, and Fig. 7 shows textures samples from the KTH database.

Vancouver image size is 9785 × 8779 pixels and has a special resolution of 1 m × 3 m. The image contains three different types of land cover: mountains, sea, and urban area. Figure 8 shows Vancouver image. Figure 9 shows the San Francisco Bay area image, which is a 900 × 1024 full polarimetric image.

5.1 Statistical modeling

In our work, Gaussian, Rayleigh, Log-Normal, Inverse-Gaussian, Weibull, and alpha-stable distributions have been used for modeling. These distributions have been chosen because they have been used

in many state of the art texture analysis publications [24, 42–45].

Maximum likelihood (ML) method has been used to estimate parameters of each distribution. Figure 10 shows the statistical modeling steps. First, the input image is decomposed using contourlet transform. Next, for each distribution, parameters are estimated using maximum likelihood method.

To evaluate how well each distribution fits the data, Kolmogorov–Smirnov distance (KSD) has been used. KSD is calculated based on Eq. 2, where CFD is the cumulative distribution function of the proposed distribution and EFD is the cumulative distribution function from image histogram.

$$ KSD = \max\{|CDF(x) - EDF(x)|\} \tag{2} $$

The estimation has been done for all the Brodatz and Vistex images and for each of the Vancouver image polarizations.

5.2 Image segmentation

Figure 11 shows the segmentation algorithm. First, additive Gaussian noise is added to the image. To evaluate the performance of each method in the presence of noise, Gaussian noise with different densities

Table 3 Standard deviation of segmentation accuracy for different methods (without noise)

|	Gaussian	Rayleigh	Alpha-stable	Contourlet + Gaussian	Contourlet + Rayleigh	Contourlet + alpha-stable	Fractal	Contourlet + Fractal	Wavelet + alpha-stable
Brodatz album	4.30E-02	2.11E-02	2.08E-02	3.87E-03	1.06E-03	1.07E-03	5.11E-02	4.32E-02	4.36E-03
Vistex Database	8.47E-02	6.06E-02	4.80E-02	3.26E-03	1.57E-03	1.27E-03	7.25E-02	6.62E-02	3.71E-03
KTH-TIPS2	2.66E-02	2.38E-02	2.36E-02	2.80E-03	1.32E-03	8.13E-04	2.57E-02	5.81E-02	3.28E-03
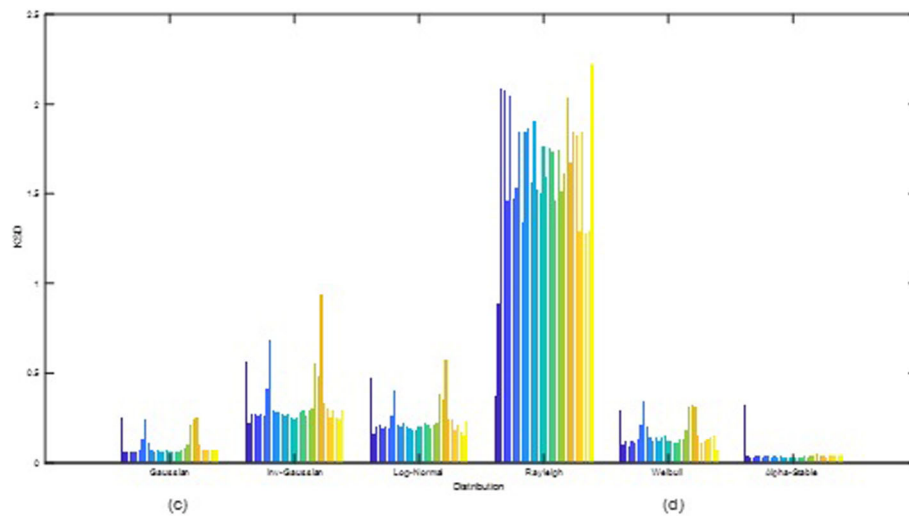
Fig. 21 Estimation results the San Francisco Bay image. Average KSD values for different distributions in each subband

has been added to the images, and segmentation has been done with various noise densities.

Next, feature extraction is performed. Different texture analysis methods have been used for feature extraction. These methods include statistical modeling and fractal analysis of the image both in the Contourlet and the image domain. Table 1 shows a summary of different feature sets.

Figure 12 shows feature extraction process in the image domain. For each pixel, a 25 × 25-pixels window has been selected around it and the features have been extracted from this window. Next, the histogram of the pixel values inside of the window is calculated and different distributions have been

fitted to this histogram. For each of the mentioned distributions, its parameters have been estimated using the maximum likelihood method and these parameters have been used as features for classification.

Figure 13 illustrates the feature extraction process in contourlet domain. First the image is transformed to the contourlet domain and the contourlet subbands are calculated. We perform a single level contourlet decomposition in five directions. This will result in 1 approximation and 32 detail images containing contourlet coefficients. Next, distribution parameters are estimated for each of the subbands.
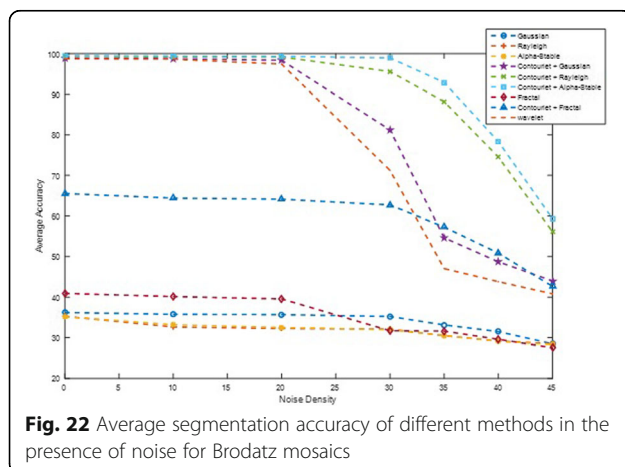

Fig. 22 Average segmentation accuracy of different methods in the presence of noise for Brodatz mosaics
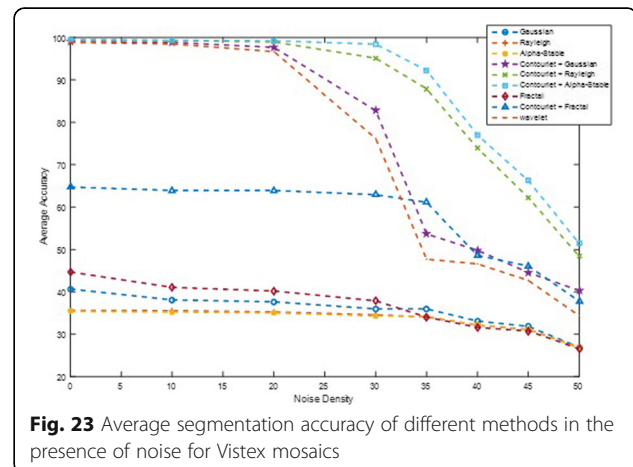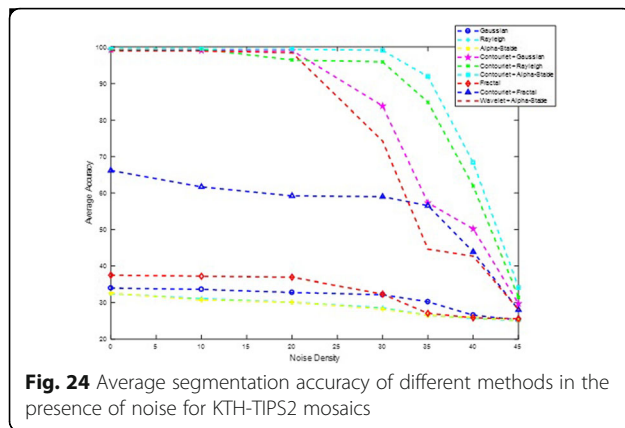

Fig. 23 Average segmentation accuracy of different methods in the presence of noise for Vistex mosaics

Fig. 24 Average segmentation accuracy of different methods in the presence of noise for KTH-TIPS2 mosaics
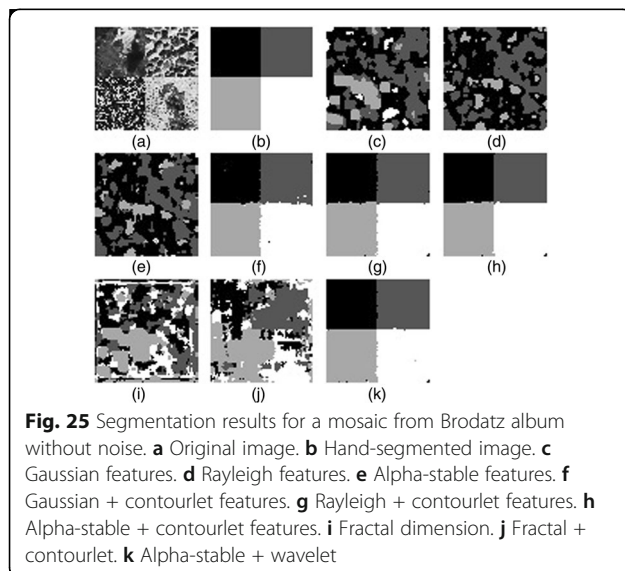
For comparison, fractal analysis which is another texture analysis method has also been used for feature extraction [20].

A three-layered perceptron neural network with 25 neurons in the hidden layer has been used as the classifier. Figure 14 shows this network's structure. Hyperbolic tangent sigmoid transfer function was used for hidden and output layers (Figs. 15).

6 Simulation results and discussion

The following figures show the estimation results. They contain average value of KSD for different distributions in each subband. Figure 16 shows the average KSD values of each sub band for the alpha-stable distribution. The first subband is the approximation image, and subband numbers 2 through 33 are the

Fig. 25 Segmentation results for a mosaic from Brodatz album without noise. **a** Original image. **b** Hand-segmented image. **c** Gaussian features. **d** Rayleigh features. **e** Alpha-stable features. **f** Gaussian + contourlet features. **g** Rayleigh + contourlet features. **h** Alpha-stable + contourlet features. **i** Fractal dimension. **j** Fractal + contourlet. **k** Alpha-stable + wavelet

detail images, which contain the texture information. From the graph, it is clear that alpha-stable distribution has the highest error in the first sub band, which is the approximation, which means this distribution is useful for modeling the texture information in the detail images.

Figures 17, 18, and 19 show comparison of the KSD values and the standard deviation of the estimation error for different distributions in each subband. We can see by obtained results, alpha-stable distribution has the lowest estimation error in the subbands representing the texture. Furthermore, the standard deviation of error in these subbands is lowest for alpha-stable distribution in most cases. Rayleigh distribution has the highest error among all the distributions. Gaussian distribution also leads to acceptable results.

In Figs. 20 and 21, we can see the estimation results for the SAR images. It is quite clear that the alpha-stable distribution is best model for representing this type of texture.

We can see that for the Brodatz textures and both SAR polarizations alpha-stable distribution has the best performance. This is due to alpha-stable distribution's ability to model both skewed and heavy tailed data.

Segmentation has been done for 100 random texture mosaics generated from each of Brodatz, Vistex, and KTH-THIPS2 databases which is a total of 300 texture mosaics. Figures 5, 6, and 7 show some samples of these mosaics. Table 2 contains the average segmentation accuracy of different methods performed on the texture mosaics and the SAR images. Considering the results, it is clear that using contourlet transform vastly improves the segmentation accuracy. This improvement is because of contourlet's ability to extract texture details in multiple scales and directions. Comparison of contourlet and wavelet's results shows the importance of analyzing the image in more than 3 directions. Therefore, texture modeling in contourlet domain can be a powerful tool for image segmentation.

Using alpha-stable distribution to model texture in contourlet domain leads to the highest segmentation accuracy among all the simulated methods. It is due to use of analyzing the texture in multiple directions and scales using contourlet, combined with alpha-stable distribution fitting the data. Table 3 shows the standard deviation of the segmentation accuracy for each method, which shows that the proposed algorithm's accuracy has the lowest standard deviation.

Figures 22, 23, and 24 plot the segmentation accuracy with different noise densities. Figures 25, 26, 27, and 28
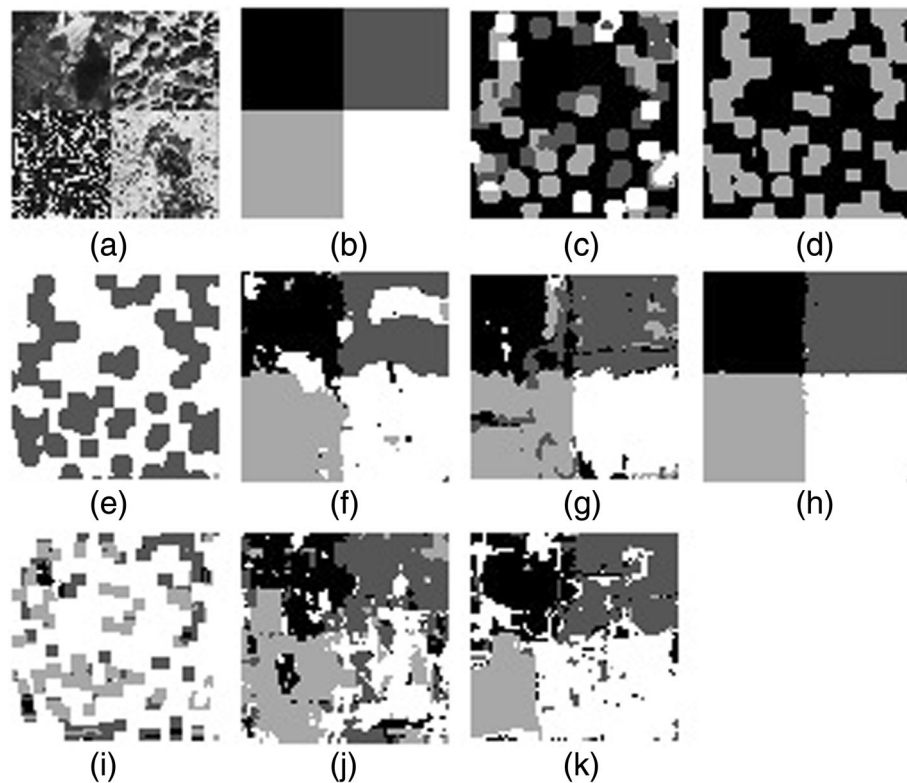
Fig. 26 Segmentation results for the previous mosaic in presence of Gaussian noise with density of 0.3. **a** Original image. **b** Hand-segmented image. **c** Gaussian features. **d** Rayleigh features. **e** Alpha-stable features. **f** Gaussian + contourlet features. **g** Rayleigh + contourlet features. **h** Alpha-stable + contourlet features. **i** Fractal dimension. **j** Fractal + contourlet. **k** Alpha-stable + wavelet

Fig. 27 Segmentation results for a mosaic from Vistex album without noise. **a** Original image. **b** Hand-segmented image. **c** Gaussian features. **d** Rayleigh features. **e** Alpha-stable features. **f** Gaussian + contourlet features. **g** Rayleigh + contourlet features. **h** Alpha-stable + contourlet features. **i** Fractal dimension. **j** Fractal + contourlet. **k** Alpha-stable + wavelet
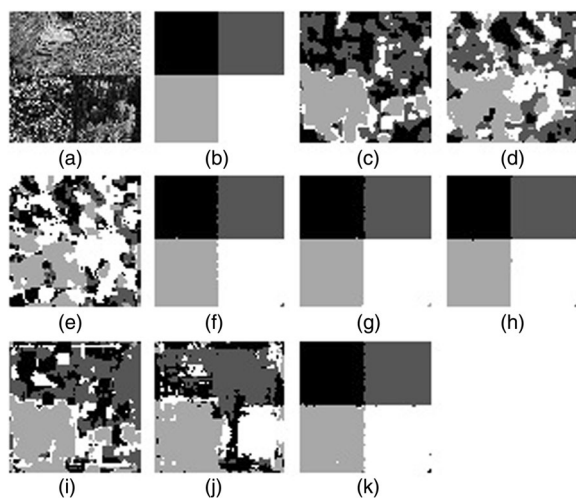

Fig. 28 Segmentation results for the previous mosaic in presence of Gaussian noise with density of 0.3. **a** Original image. **b** Hand-segmented image. **c** Gaussian features. **d** Rayleigh features. **e** Alpha-stable features. **f** Gaussian + contourlet features. **g** Rayleigh + contourlet features. **h** Alpha-stable + contourlet features. **i** Fractal dimension. **j** Fractal + contourlet. **k** Alpha-stable + wavelet
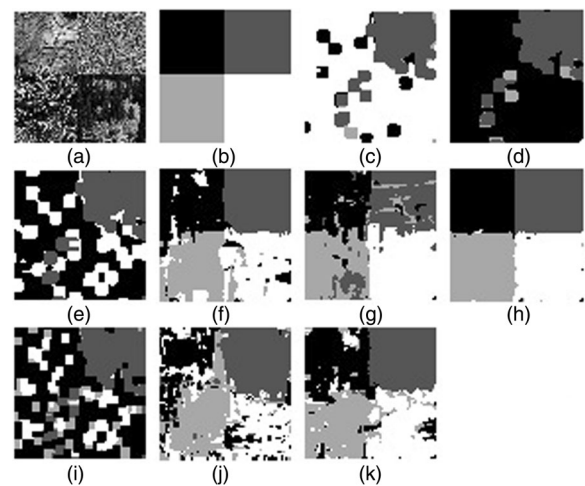
Fig. 29 Segmentation results for Vancouver image. **a** Original image. **b** Hand-segmented image. **c** Gaussian features. **d** Rayleigh features. **e** Alpha-stable features. **f** Gaussian + contourlet features. **g** Rayleigh + contourlet features. **h** Alpha-stable + contourlet features. **i** Fractal dimension. **j** Fractal + contourlet. **k** Alpha-stable+ wavelet
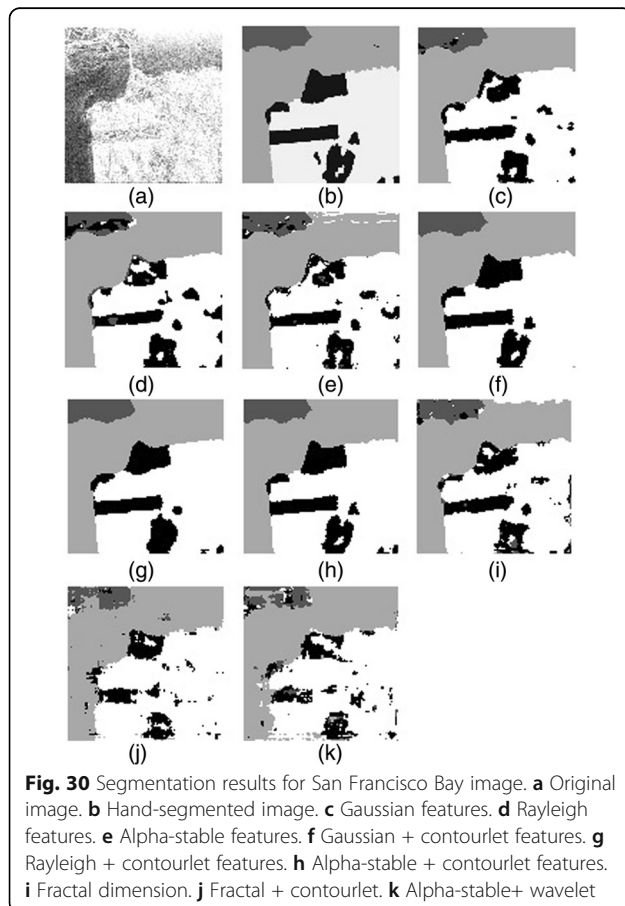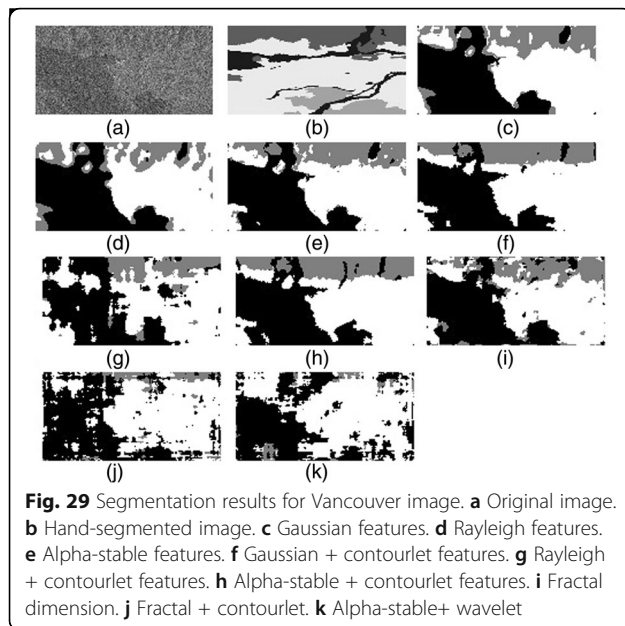

Fig. 30 Segmentation results for San Francisco Bay image. **a** Original image. **b** Hand-segmented image. **c** Gaussian features. **d** Rayleigh features. **e** Alpha-stable features. **f** Gaussian + contourlet features. **g** Rayleigh + contourlet features. **h** Alpha-stable + contourlet features. **i** Fractal dimension. **j** Fractal + contourlet. **k** Alpha-stable+ wavelet

show also the segmentation results for some sample images with and without noise. We can see that the proposed method is also very robust in the presence of noise. As a matter of fact, even though Gaussian and Rayleigh modeling produce acceptable results in case of the noise free case, their performance drops significantly in the presence of noise (Figs. 29 and 30).

7 Conclusion

In this paper, skewed alpha stable distribution has been proposed for modeling the contourlet subbands of textured images. Simulation results show that alpha stable distribution can model the textured data in contourlet domain better than other distributions. This is due to alpha-stable distribution's ability to model a wide range of data combined of different histogram shapes. Since contourlet transform provides texture details in multiple directions, statistical modeling of these details can be used as an effective method for texture feature extraction and classification.

We have also proposed a new texture segmentation method based on alpha-stable distribution parameters in contourlet domain. The performance of the proposed features on image segmentation has been compared with that of features extracted using Gaussian and Rayleigh distributions and fractal features which have been used in earlier texture segmentation works. Results have demonstrated the superior performance of new features in segmentation of textured images.

Even though Gaussian and Rayleigh parameters of contourlet domain perform almost as well as the alpha-stable features for the noise-free case, as the noise density increases their segmentation accuracy decreases quickly. The proposed segmentation method has the best accuracy and is the most robust in the presence of noise.

Publisher's Note

Author details
[1]Shiraz University, Shiraz, Iran. [2]Electrical Engineering Department, Shiraz university, Shiraz, Iran.

References
1. M. Petrou, P. García Sevilla, *Image processing: dealing with texture* (2006)
2. X. Liu, D. Wang, Texture classification using spectral histograms. IEEE Trans. Image Process. **12**(6), 661–670 (2003)
3. C. Sagiv, N.A. Sochen, Y.Y. Zeevi, Integrated active contours for texture segmentation. IEEE Trans. Image Process. **15**(6), 1633–1646 (2006)
4. M. Varma, A. Zisserman, A statistical approach to material classification using image patch exemplars. IEEE Trans. Pattern Anal. Mach. Intell. **31**(11), 2032–2047 (2009)
5. Y. Xia, D. Feng, R. Zhao, Adaptive segmentation of textured images by using the coupled Markov random field model. IEEE Trans. Image Process. **15**(11), 3559–3566 (2006)
6. M. Ponti, T.S. Nazaré, G.S. Thumé, Image quantization as a dimensionality reduction procedure in color and texture feature extraction. Neurocomputing **173**, 385–396 (2016)
7. A. Anandh, K. Mala, S. Suganya, *Content based image retrieval system based on semantic information using color, texture and shape features*, In 2016 International Conference on Computing Technologies and Intelligent Data Engineering (ICCTIDE'16) (IEEE, India, 2016), pp. 1–8
8. P. Yang, Z. Hou, X. Liu, Z. Shi, *Texture feature extraction of mountain economic forest using high spatial resolution remote sensing images*, In 2016 IEEE International Geoscience and Remote Sensing Symposium (IGARSS) (pp. 3156–3159) (IEEE, China, 2016)
9. C. Yan et al., Effective Uyghur language text detection in complex background images for traffic prompt identification. IEEE Trans Intell Transp Sys **19**(1), 220–229 (2018)
10. R.M. Haralick, K. Shanmugam, Textural features for image classification. IEEE Transactions on Systems, Man, and Cybernetics (6), 610–621 (1973)
11. B. Khaldi, M.L. Kherfi, Modified integrative color intensity co-occurrence matrix for texture image representation. Journal of Electronic Imaging **25**(5), 053007–053007 (2016)
12. I. Pantic et al., Fractal analysis and gray level co-occurrence matrix method for evaluation of reperfusion injury in kidney medulla. J. Theor. Biol. **397**, 61–67 (2016)
13. R.C. Geary, The contiguity ratio and statistical mapping. The Incorporated Statistician **5**(3), 115–146 (1954)
14. P.A. Moran, Notes on continuous stochastic phenomena. Biometrika **37**(1/2), 17–23 (1950)
15. N. Ahuja, Dot pattern processing using Voronoi neighborhoods. IEEE Trans. Pattern Anal. Mach. Intell. **3**, 336–343 (1982)
16. Y. Qiao, G. Zhao, in *Advanced Multimedia and Ubiquitous Engineering*, Lecture Notes in Electrical Engineering, ed. by J. Park, H. Jin, Y. S. Jeong, M. Khan. Modified Wavelet Domain Hidden Tree Model for Texture Segmentation, vol 393 (Springer, Singapore, 2016)
17. S.Z. Li, *Markov random field modeling in image analysis* (Springer Science & Business Media, 2009)
18. S. Sturtz, H. Rue, L. Held, Gaussian Markov random fields. Theory and applications. Metrika **67**(2), 243–244 (2008)
19. Q.-h. Zhao et al., A fuzzy clustering image segmentation algorithm based on hidden Markov random field models and Voronoi tessellation. Pattern Recogn. Lett. **85**, 49–55 (2017)
20. K. Sarafrazi, M. Yazdi, M.J. Abedini, A new image texture segmentation based on contourlet fractal features. Arab. J. Sci. Eng. **38**(12), 3437–3449 (2013)
21. C. Yan et al., A highly parallel framework for HEVC coding unit partitioning tree decision on many-core processors. IEEE Signal Processing Letters **21**(5), 573–576 (2014)
22. C. Yan et al., Efficient parallel framework for HEVC motion estimation on many-core processors. IEEE Transactions on Circuits and Systems for Video Technology **24**(12), 2077–2089 (2014)
23. R.A. Ansari, K.M. Buddhiraju, *Textural classification based on wavelet, curvelet and contourlet features*, In 2016 IEEE International Geoscience and Remote Sensing Symposium (IGARSS) (IEEE, 2016), pp. 2753–2756
24. S. Susan, M. Sharma, Automatic texture defect detection using Gaussian mixture entropy modeling. Neurocomputing **239**, 232–237 (2017)
25. P. Lévy, Théorie des erreurs. La loi de Gauss et les lois exceptionnelles. Bulletin de la Société mathématique de France **52**, 49–85 (1924)
26. Y.D. Cid, H. Müller, A. Platon, P.A. Poletti, A. Depeursinge, 3D solid texture classification using locally-oriented wavelet transforms. IEEE Transactions on Image Processing **26**(4), 1899–1910 (2017)
27. C. Li, Y. Huang, L. Zhu, Color texture image retrieval based on Gaussian copula models of Gabor wavelets. Pattern Recogn. **64**, 118–129 (2017)
28. Z. Tirandaz, G. Akbarizadeh, A two-phase algorithm based on kurtosis curvelet energy and unsupervised spectral regression for segmentation of SAR images. IEEE Journal of Selected Topics in Applied Earth Observations and Remote Sensing **9**(3), 1244–1264 (2016)
29. M.N. Do, M. Vetterli, Wavelet-based texture retrieval using generalized Gaussian density and Kullback-Leibler distance. IEEE Trans. Image Process. **11**(2), 146–158 (2002)
30. E. de Ves et al., A statistical model for magnitudes and angles of wavelet frame coefficients and its application to texture retrieval. Pattern Recogn. **47**(9), 2925–2939 (2014)
31. M.S. Allili, N. Baaziz, M. Mejri, Texture modeling using contourlets and finite mixtures of generalized Gaussian distributions and applications. IEEE Transactions on Multimedia **16**(3), 772–784 (2014)
32. M.N. Do, M. Vetterli, The contourlet transform: An efficient directional multiresolution image representation. IEEE Trans. Image Process. **14**(12), 2091–2106 (2005)
33. B.S. Manjunath, W.-Y. Ma, Texture features for browsing and retrieval of image data. IEEE Trans. Pattern Anal. Mach. Intell. **18**(8), 837–842 (1996)
34. M.S. Allili, Wavelet modeling using finite mixtures of generalized Gaussian distributions: application to texture discrimination and retrieval. IEEE Trans. Image Process. **21**(4), 1452–1464 (2012)
35. H. Rami et al., Texture retrieval using mixtures of generalized Gaussian distribution and Cauchy–Schwarz divergence in wavelet domain. Signal Process. Image Commun. **42**, 45–58 (2016)
36. R. Kwitt, A. Uhl, Lightweight probabilistic texture retrieval. IEEE Trans. Image Process. **19**(1), 241–253 (2010)
37. S.-K. Choy, C.-S. Tong, Statistical wavelet subband characterization based on generalized gamma density and its application in texture retrieval. IEEE Trans. Image Process. **19**(2), 281–289 (2010)
38. A.D. El Maliani, M. El Hassouni, N. Lasmar, Y. Berthoumieu, *Texture classification based on the generalized gamma distribution and the dual tree complex wavelet transform*, In 2010 5th International Symposium On I/V Communications and Mobile Network (IEEE, Morocco, 2010), pp. 1–4
39. S. Mallat, *A wavelet tour of signal processing* (Elsevier, 1999)
40. P. Brodatz, *Textures: a photographic album for artists and designers* (Dover Pubns, 1966)
41. P. Mallikarjuna et al., *The kth-tips2 database* (Computational Vision and Active Perception Laboratory (CVAP), Stockholm, Sweden, 2006)
42. H. Isono, S. Hirata, H. Hachiya, Quantitative analysis of ultrasonic images of fibrotic liver using co-occurrence matrix based on multi-Rayleigh model. Jpn. J. Appl. Phys. **54**(7S1), 07HF15 (2015)
43. Vacher, J., et al. Biologically inspired dynamic textures for probing motion perception. in Advances in Neural Information Processing Systems. 2015
44. S.-W. Xu, J. Xue, P.-L. Shui, Adaptive detection of range-spread targets in compound Gaussian clutter with the square root of inverse Gaussian texture. Digital Signal Processing **56**, 132–139 (2016)
45. A.D. El Maliani et al., Color texture classification method based on a statistical multi-model and geodesic distance. J. Vis. Commun. Image Represent. **25**(7), 1717–1725 (2014)
46. C. Dharmagunawardhana et al., Gaussian Markov random field based improved texture descriptor for image segmentation. Image Vis. Comput. **32**(11), 884–895 (2014)